Supporting Information

Sustained Water Oxidation with Surface- and Interface-Engineered $WO_3/BiVO_4$ Heterojunction Photoanodes

Hasmat Khan[1,2], Min-Ji Kim[1], Ji-Hu Baek[1], Susanta Bera[1,2], Hyun-Jae Woo[1], Hyoung-Seok Moon[3] and Se-Hun Kwon[1,2]*

[1]School of Materials Science and Engineering, Pusan National University, Busan 46241, Republic of Korea

[2]Institute of Materials Technology, Pusan National University, Busan 46241, Republic of Korea

[3]Advanced Energy Materials and Engineering R&D Group, Korea Institute of Industrial Technology (KITECH), Busan 46938, Republic of Korea

*Correspondence: sehun@pusan.ac.kr (S.-H. Kwon)

Contents

Section I

Calculations for photoelectrochemical processes:

Light harvesting efficiency (LHE) of the respective photoanodes were calculated from defuse reflectance and transmittance by the following equation (1)

$$LHE\ (\%) = 100\ (\%) - R\ (\%) - T\ (\%) \quad \text{---------- (1)}$$

The absorption photocurrents (J_{abs}) of the samples were estimated by integrating photon flux and LHE over the wavelength (λ) 300 nm to 510 nm, eq. (2)

$$J_{abs} = \int_{\lambda 1}^{\lambda 2} Photon\ \ flux \times LHE \times d\lambda \quad \text{---------- (2)}$$

Theoretical maximum photocurrent (J_{max}) was calculated considering 100 % incident photon to current conversion efficiency (IPCE) by the eq. (3)

$$J_{max} = \int_{\lambda 1}^{\lambda 2} Photon\ \ flux \times IPCE \times electron\ \ charge \times d\lambda \quad \text{---- (3)}$$

Absorption efficiency, $\eta_{abs} = \frac{J_{abs}}{J_{max}}$ ---------- (4)

Theoretical Photocurrent for water oxidation (J_{H_2O}) is expressed in eq. (5)

$$J_{H_2O} = J_{max} \times \eta_{abs} \times \eta_{sep} \times \eta_{trans} \quad \text{---------- (5)}$$

In sulfite oxidation reaction, charge transfer efficiency (η_{trans}) is around 100 % due to fast oxidation by the photogenerated holes.

Assuming, $\eta_{trans} = 100\%$, the product of absorption efficiency and charge separation efficiency (η_{abs} x η_{sep}) was calculated from equ. (5)

$$\eta_{abs} \times \eta_{sep} = \frac{J_{water}}{J_{max}} \quad \text{---------- (6)}$$

$$\eta_{sep} = \frac{J_{water}}{J_{max} \times \eta_{abs}} \quad \text{---------- (7)}$$

The charge transfer efficiency (η_{trans}) was calculated from eq. (8)

$$\eta_{trans} = \frac{J_{water}}{J_{sulfite}} \quad \text{---------- (8)}$$

Section II

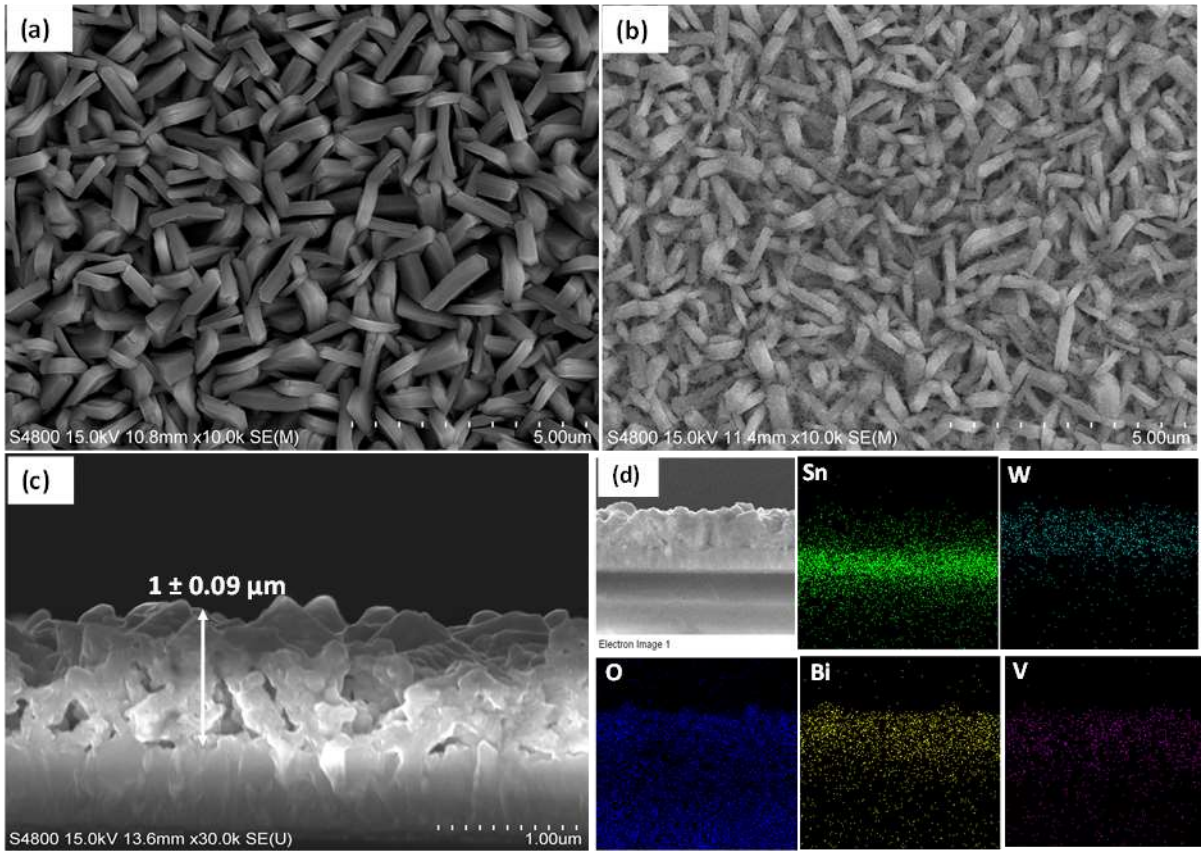

Figure S1. Top view SEM images of (a,b) pristine WO_3, and WBV films. (c,d) cross-sectional SEM images of WBV film deposited onto FTO substrate with corresponding elemental mapping shows the presence of Sn, W, O, Bi and V elements.

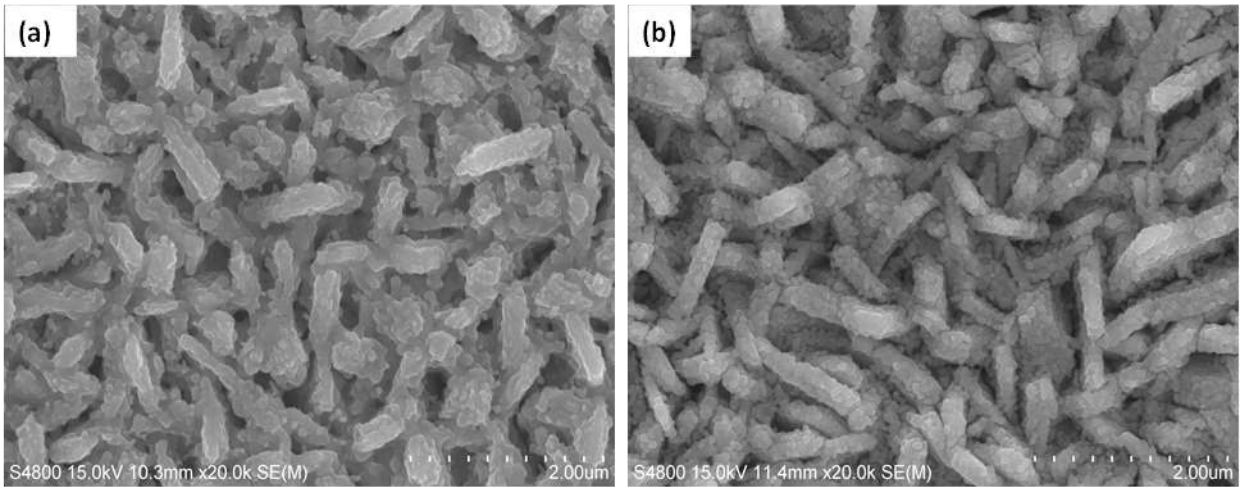

Figure S2. Top view SEM images of (a) WBV film without Pluronic P123 (organic triblock co-polymer) and (b) WBV film with Pluronic P123 shows less agglomeration of $BiVO_4$ nanoparticles attached on WO_3 nanosheets.

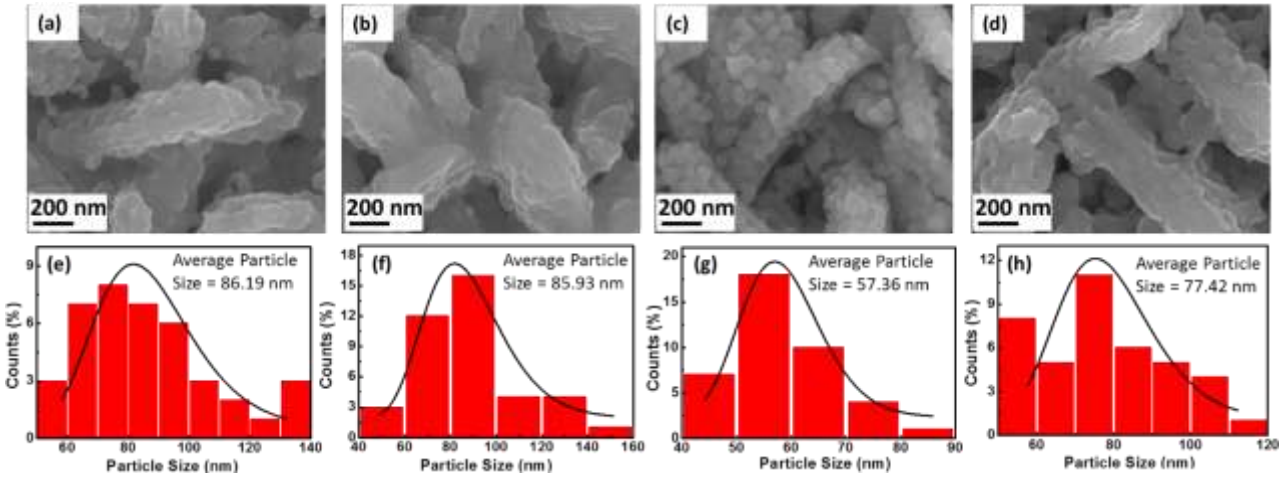

Figure S3. Top view SEM images of WBV films with different amount of Pluronic P123; (a) 0 mg, (b) 5 mg, (c) 10 mg, (d) 15 mg and (e-h) the particle size distribution curves obtained from the corresponding SEM images.

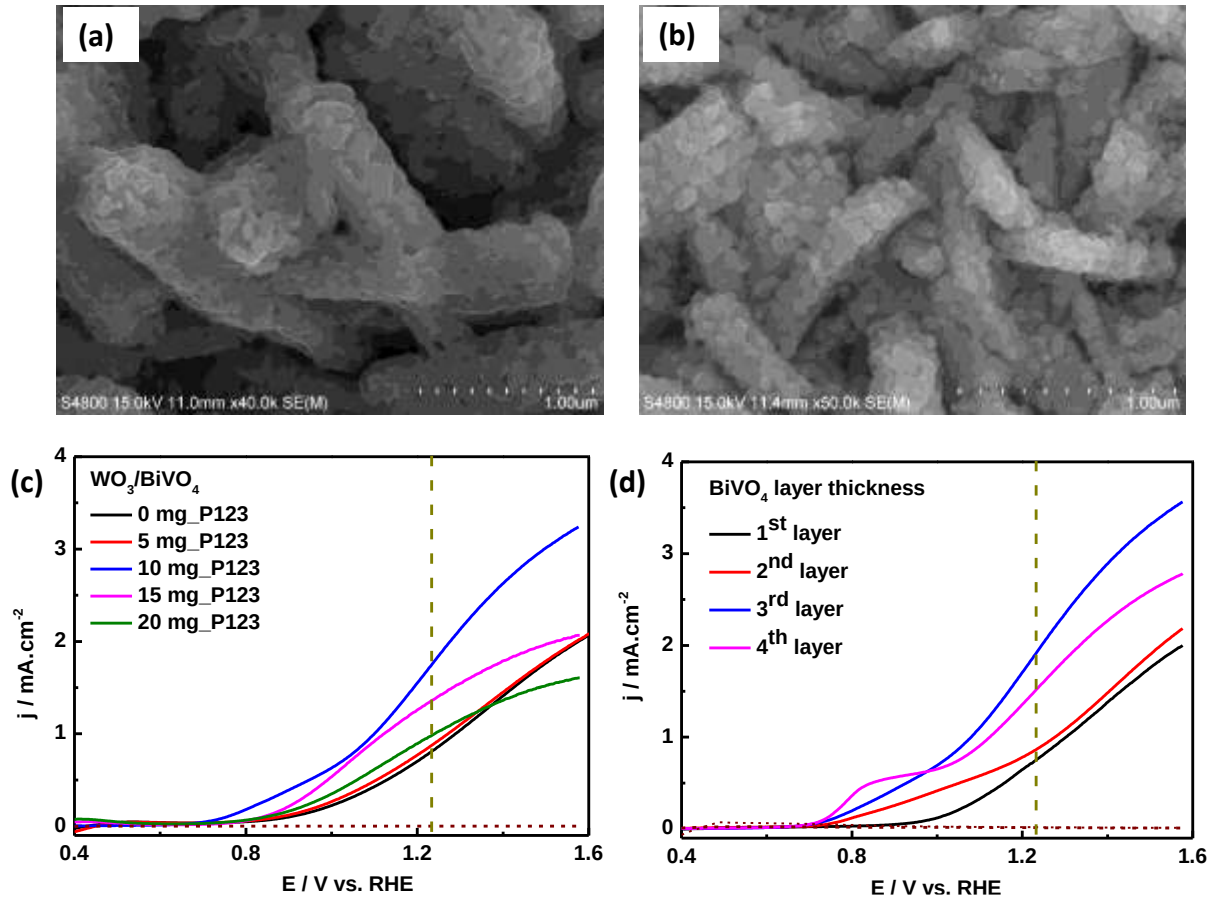

Figure S4. Top view SEM images of WBV films with different $BiVO_4$ layer thicknesses on

WO_3 nanosheets (a) 4th layer and (b) 3rd layer. (c,d) the LSV curves of WBV films with different amount of Pluronic P123 and different $BiVO_4$ loading, respectively.

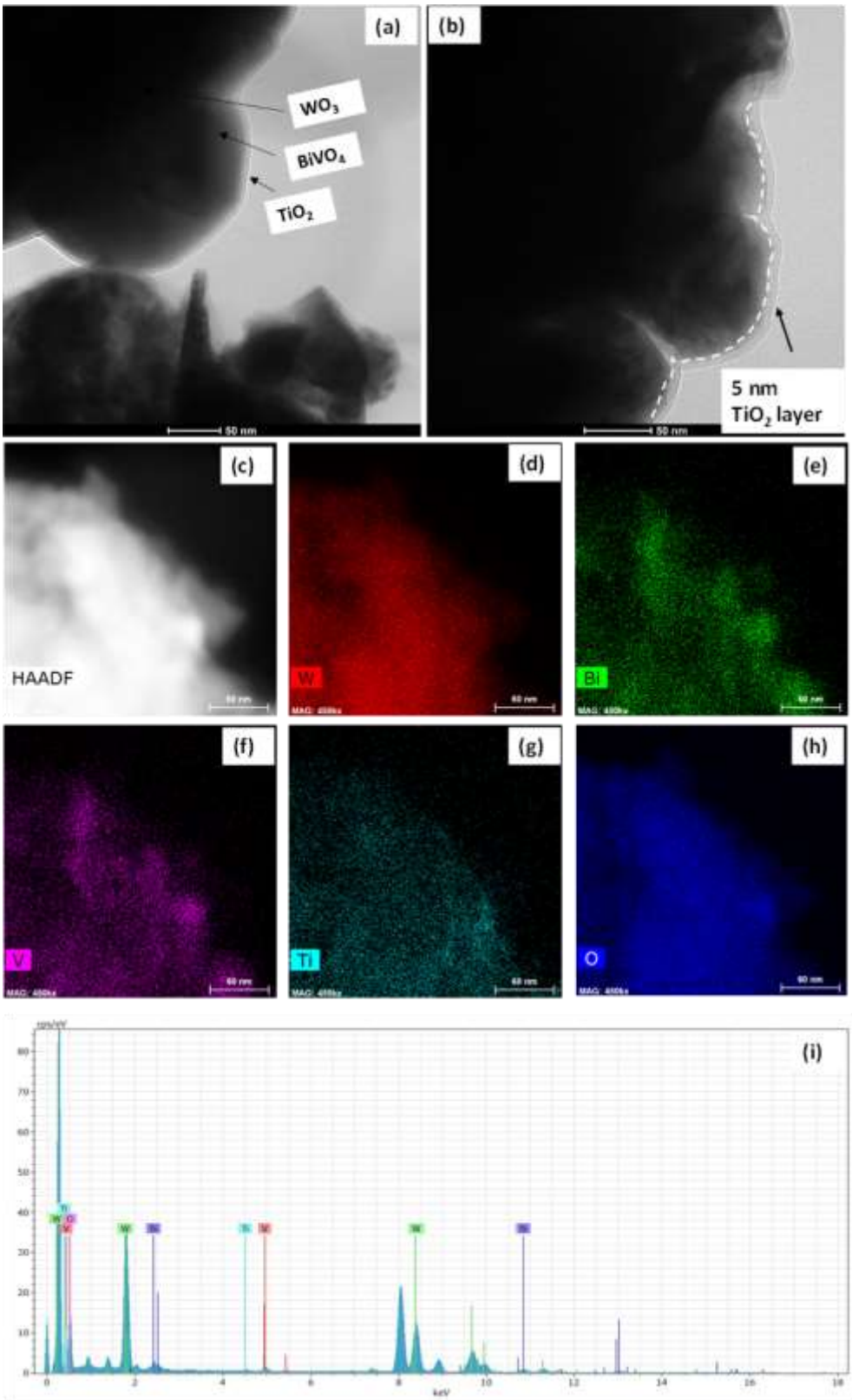

Figure S5. TEM study of WBV film coated with 50 cycle ALD TiO_2; (a,b) bright field TEM images showing the amorphous TiO_2 layer (~ 5 nm) closely attached to the $BiVO_4$ particle and

(c-i) the TEM-EDS and mapping studies reveal the presence of W, Bi, V, Ti and O elements, respectively.

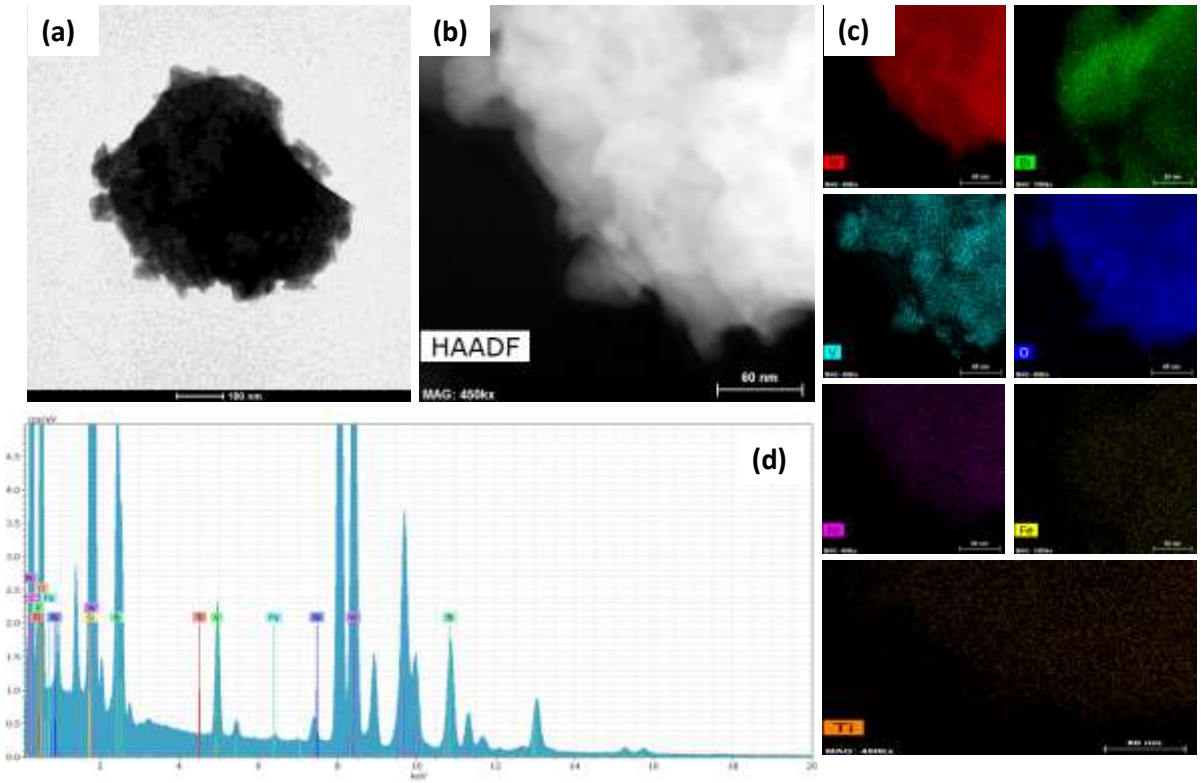

Figure S6. TEM studies of WBVT/cocat. sample; (a) bright field TEM image, (b,c) HAADF image shows the elemental mapping images of different constituent elements, (d) TEM- EDS spectra also confirm the presence of W, Bi, V, Ti, Fe, Ni and O elements in the film matrix.

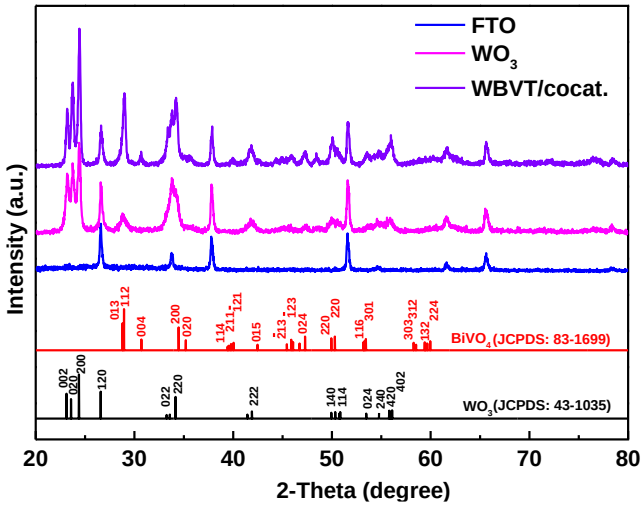

Figure S7. X-ray diffraction study of WO3 and WBVT/cocat. photoanodes

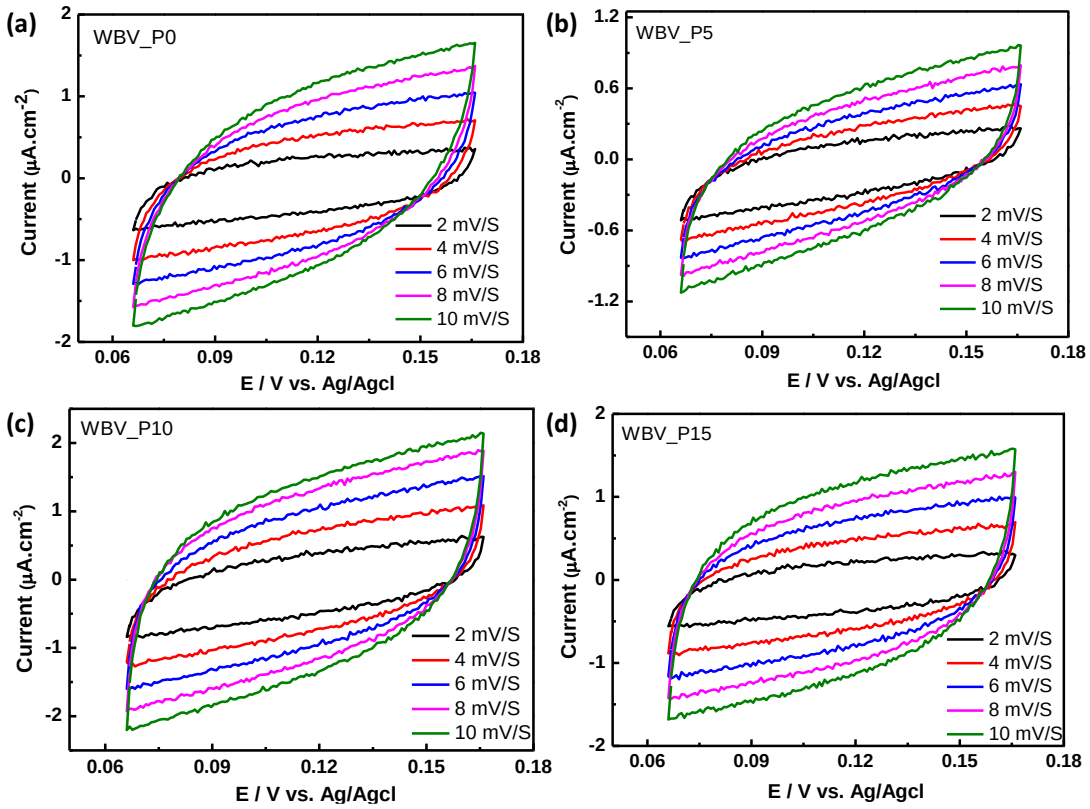

Figure S8. Measurement of cyclic voltammetry at different scan rates within a potential window range from 0.066 to 0.166 V vs Ag/AgCl for WBV electrodes with different amount of Pluronic P123 (a) WBV_P0, (b) WBV_P5, (c) WBV_P10 and (d) WBV_P15.

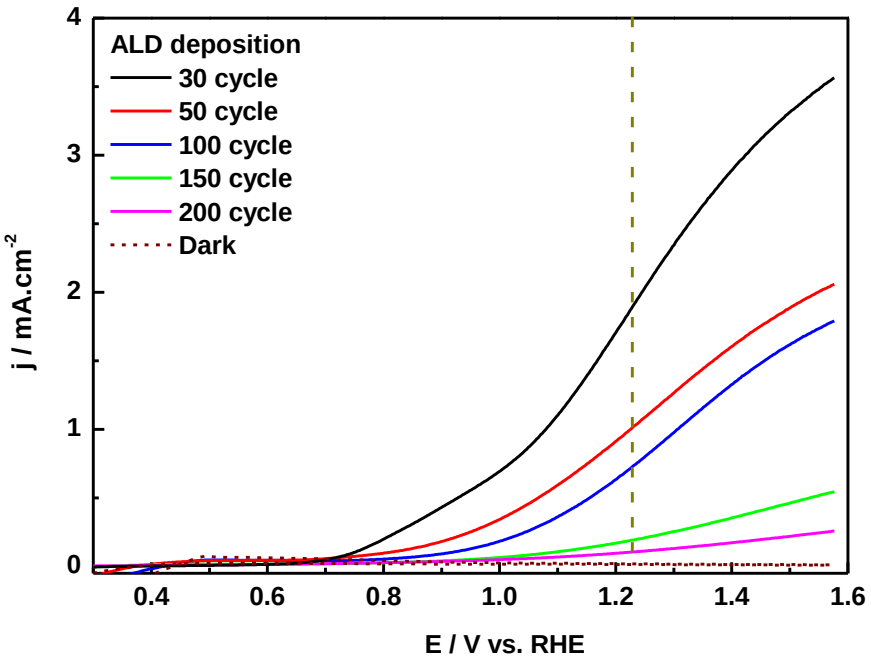

Figure S9. The LSV curves of WBV samples with different TiO_2 layer thicknesses by varying ALD cycle numbers.

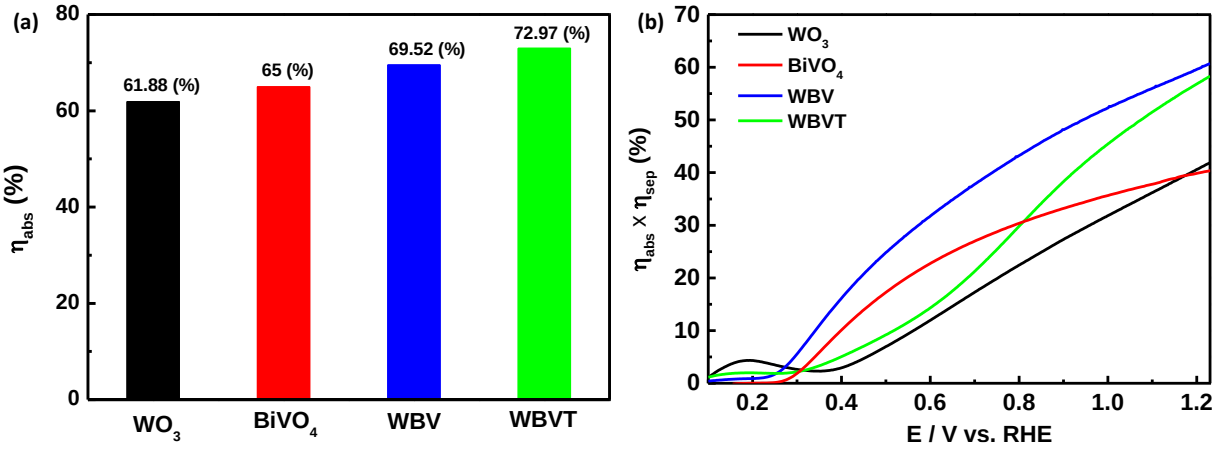

Figure S10. (a) Absorption efficiency (η_{abs}, calculated by dividing the absorption photocurrent by J_{max}) of the respective samples (b) $\eta_{abs} \times \eta_{sep}$ curve of different photoanodes.

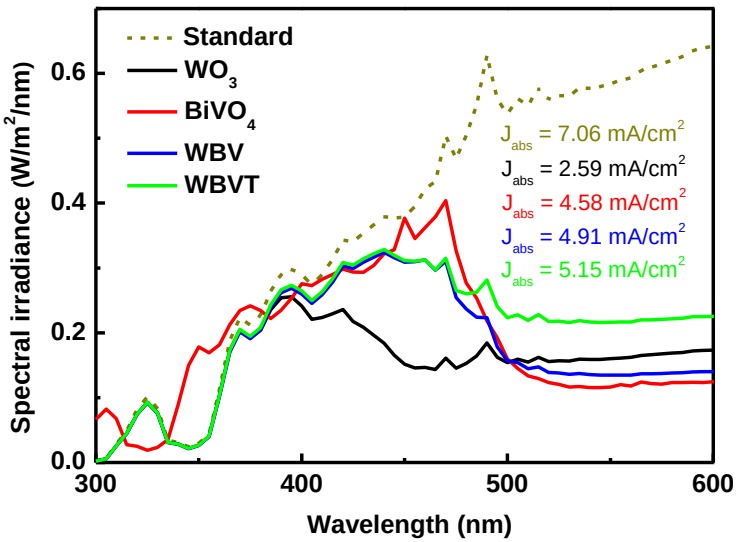

Figure S11. Spectra of the solar irradiance of AM 1.5G and calculated J_{abs} obtained from LHE spectra of WO_3, $BiVO_4$, WBV and WBVT photoanodes in the wavelength range 300 nm to 600 nm.

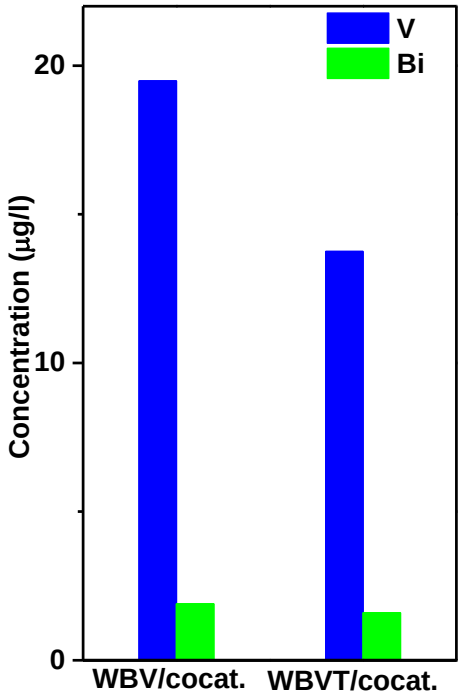

Figure S12. Inductively Coupled Plasma–Mass Spectrometry (ICP–MS) analyses of the electrolyte after the long-term stability (J–t measurement) of 24h for WBV/cocat. and WBVT/cocat. photoanodes.

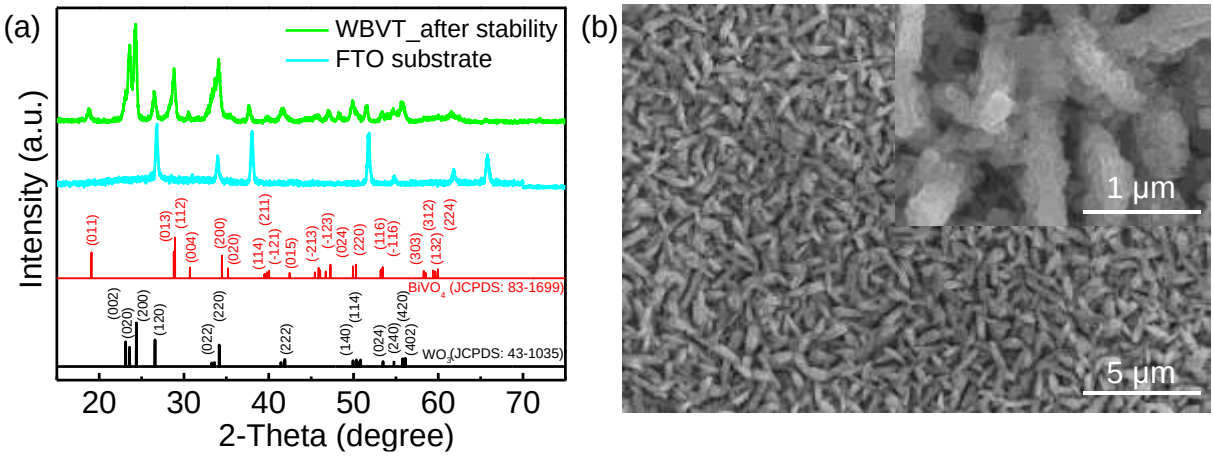

Figure S13: (a) X-ray diffraction study and (b) SEM image of the TiO_2 layer coated $WO_3/BiVO_4$ heterojunction photoanode after stability test. Inset of (b) represents the high magnified SEM image.

Table S1. Comparison of photocurrent densities for different state-of-the-art $WO_3/BiVO_4$ photoanodes

Materials	**Light intensity ($mWcm^{-2}$)**	**Electrolyte**	**Photocurrent density ($mAcm^{-2}$)**	**Ref.**
$WO_3/BiVO_4$	100	0.5 M Na_2SO_4	1.7 $mAcm^{-2}$ (0.7 V vs. Ag/AgCl)	*Energy Environ. Sci. 4 (2011) 1781–1787*
WO3/BiV0.95 Mo0.05O4	100	0.5 M Na_2SO_4	1.7 $mAcm^{-2}$ (1.23 V vs. RHE)	*Phys. Chem. Chem. Phys. 14 (2012) 11119–11124*
$WO_3/BiVO_4$	100	0.5 M Na_2SO_4	1 $mAcm^{-2}$ (1.23 V vs. RHE)	*J. Phys. Chem. C 119 (2015) 20792−20800*
$WO_3/BiVO_4$	100	0.5 M Na_2SO_4 + 0.1 M K_2HPO_4 buffer	~1.5 $mAcm^{-2}$ (1.6 V vs. RHE)	*J. Phys. Chem. C 117 (2013) 21635−21642*
$WO_3/BiVO_4$	100	0.5M Na_2SO_4	1.5 $mAcm^{-2}$ (1.0 V vs. NHE)	*Nano Lett. 11 (2011) 1928–1933*
$WO_3/BiVO_4$	100	0.1 M KH_2PO_4	~1.1 $mAcm^{-2}$ (2.0 V vs. RHE)	*ACS Appl. Mater. Interfaces 9 (2017) 19780−19790*
$WO_3/BiVO_4$	100	0.5 M Na_2SO_4	~1.4 $mAcm^{-2}$ (1.5 V vs. RHE)	*ACS Energy Lett. 2 (2017) 1362−1367*
WO_3/W-Mo $BiVO_4$	100	0.1M Na_2SO_4 + K_2HPO_4 buffer	1.48 $mAcm^{-2}$ (0.6V vs. Ag/AgCl)	*J. Electroanal. Chem. 789 (2017) 17–23*
$WO_3/BiVO_4$	100	0.5 M Na_2SO_4	0.5 $mAcm^{-2}$ (1.2 V vs. SCE)	*Solar Energy 144 (2017) 604–611*
$WO_3/BiVO_4$	100	0.5 M Na_2SO_4	0.57 $mAcm^{-2}$ (1.0V vs. Ag/AgCl)	*NPG Asia Materials 9 (2017) e357*
E-$WO_3/BiVO_4$	100	0.5 M Na_2SO_4	1.6 $mAcm^{-2}$ (1.41V vs. RHE)	*CrystEngComm. 18 (2016) 8961–8970*
$WO_3/BiVO_4$(F)	100	0.5 M Na_2SO_4	1.08 $mAcm^{-2}$ (1.41V vs. RHE)	*RSC Adv. 6 (2016) 27557–27565*
$WO_3/BiVO_4$	**100**	**0.5 M Na_2SO_4**	**1.9 $mAcm^{-2}$ (1.23 V vs. RHE)**	**This work**

Table S2: Summary of TiO_2 layer thicknesses and the stability of different $BiVO_4$-based photoanodes

Photoelectrodes	TiO_2 thickness (nm)	Photostability	References
$WO_3/BiVO_4/ALD\text{-}TiO_2$/ FeOOHNiOOH	**2.2 (ALD deposition)**	**24 h (4.6 mA/cm^2 at 1.23 V_{RHE})**	**Present work**
Mo:$BiVO_4$/Nb:TiO_2/ Fe:NiO co-catalyst	2.5 (ALD deposition)	16 h (5.6 mA/cm^2 at 1.23 V_{RHE})	*Adv. Funct. Mater.* **2021**, *31* (45), 2011 210
Black-$BiVO_4/TiO_{2-x}$	4 (ALD deposition)	100 h (6.1 mA/cm^2 at 1.23 V_{RHE})	*Adv. Energy Mater.* **2019**, *9*, 1901287
$BiVO_4/TiO_2$/ FeOOH/NiOOH OECs	6 (electrochemical deposition)	40 h (2.5 mA/cm^2 at 0.6 V_{RHE})	*Chem. Mater*. **2018**, *30* (14), 4704−4712
$WO_3/BiVO_4$/ TiO_2	5.5 (electrochemical deposition)	25 h (4.2 mA/cm^2 at 1.23 V_{RHE})	*J. Mater. Chem. A* **2017**, *5*, 1455–1461
R-TiO_2@$BiVO_4$	5 (ALD deposition)	6 h (2.1 mA/cm^2 at 1.23 V_{RHE})	*ACS Catal*. ***2021***, *1 1 (13), 7637−7646*

Table S3. Comparison of Charge separation (η_{sep}) and Charge transfer (η_{trans}) efficiencies at 1.23 V vs. RHE for different $WO_3/BiVO_4$ based photoanodes

Electrode materials	**Light intensity (mWcm^{-2})**	**Charge separation (η_{sep}) at 1.23 V vs. RHE**	**Charge transfer (η_{trans}) at 1.23 V vs. RHE**	**Ref.**
WO_3/ $BiVO_4$/ZnO	100	84.1 %	75 %	*ACS Appl. Mater. Interfaces 11 (2019) 889−897*
$WO_3/BiVO_4$	100	74.0 %	-------	*ACS Appl. Energy Mater. 2 (2019), 4535−4543*
$WO_3/BiVO_4$	100	76 %	77%	*Chem. Eng. J. 399 (2020) 125836*
WO_3/W:$BiVO_4$	100	77 %	79%	*Nano Lett. 14 (2014) 1099−1105*
$BiVO_4/WO_3/SnO_2$	100	93 %	85 %	*ACS Appl. Mater. Interfaces 9 (2017) 1479−1487*

$WO_3/BiVO_4$	--------	24 %[a]	45 %	*ACS Appl. Mater. Interfaces 9 (2017) 19780−19790*
Y-$WO_3/BiVO_4$/ OER	100	---------	85 %	*J. Mater. Chem. A 6 (2018) 2585–2592*
WO_3–$BiVO_4$-3(S)	100	8 %[a]	70 %	*RSC Adv. 6 (2016) 27557–27565*
002-$WO_3/BiVO_4$	100	---------	70 %[a]	*Appl. Catal. B: Environ. 245 (2019) 227–239*
$WO_3/BiVO_4$	100	88 %	54 %	Appl. Catal. B: Environ. 293 (2021) 120217
$WO_3/BiVO_4/TiO_2$/ FeOOHNiOOH	**100**	**90 %**	**95 %**	**This work**

[a] *Estimated from reported current-voltage and η_{sep}-voltage curves*

Table S4. Comparison of photocurrent density and stability for different cocatalyst deposited $WO_3/BiVO_4$ photoanodes

Materials	Light Source/ intensity	Electrolyte	Photocurrent density	Stability	Ref.
$WO_3/BiVO_4$/TANiFe	100 $mWcm^{-2}$	0.5 M Borate buffer, pH= 8.5	3.7 $mAcm^{-2}$ 1.23 V vs. RHE	5 h	*ACS Sustainable Chem. Eng. 8 (2020) 12637−12645*
WO_3/S:$Bi2O_3$/ (Ga,W):$BiVO_4$/Co-Pi	Simulated AM 1.5G illumination	0.1 M KPi pH = 8.0	5.1 $mAcm^{-2}$ 1.23 V vs. RHE	10 h	*J. Mater. Chem. A 9 (2021) 16137–16149*
Co-Pi@ $BiVO_4/WO_3$	100 $mWcm^{-2}$	0.1 M KPi pH = 7	1.8 $mAcm^{-2}$ at 1.23 V vs. RHE	0.3 h	*ACS Appl. Mater. Interfaces 11 (2019) 5623−5631*
$TiO_2/WO_3/BiVO_4$/ FeOOH/NiOOH	AM 1.5G illumination	0.5 M Na_2SO_4	4.27 $mAcm^{-2}$ 1.23 V vs. RHE	5 h	*Small 15 (2019) 1900924*
$WO_3/BiVO_4$/Co-Pi	300 W xenon lamp	0.5 M Na_2SO_4 +0.1 M KH_2PO_4	3.3 $mAcm^{-2}$ 1.23 V vs. RHE	0.5h	*J. Mater. Chem. A 2 (2014) 11408–11416*
WO_3/Mo-$BiVO_4$/Co-Pi	100 $mWcm^{-2}$	0.5 M K_2SO_4	5.38 $mAcm^{-2}$ 1.23 V vs. RHE	3 h	*Appl. Catal. B: Environ.*

					217 (2017) 21–29
$WO_3/BiVO_4$/Co-Pi	300 W xenon lamp 100 $mWcm^{-2}$	0.5 M Na_2SO_4 + KPi	2.5 $mAcm^{-2}$ 1.23 V vs. RHE	24 h	*Phys. Chem. Chem. Phys. 15 (2013) 14723–14728*
WO_3/ $BiVO_4$/CoPi	100 $mWcm^{-2}$	0.5 M Na_2SO_4	3.0 $mAcm^{-2}$ 1.23 V vs. RHE	1.4 h	**s**mall *10 (*2014) 3692–3699
$WO_3/BiVO_4$/ FeOOH/NiOOH	100 $mWcm^{-2}$	0.5 M Na_2SO_4	5.0 $mAcm^{-2}$ 1.23 V vs. RHE	0.5 h	J. Mater. Chem. A 6 (2018) 2585–2592
$WO_3/BiVO_4$/Co-Pi	100 $mWcm^{-2}$	0.5 M Na_2SO_4	4.5 $mAcm^{-2}$ 1.2 V vs. Ag/AgCl	------	*small 13 (2017) 1603840*
(WO3/BiVO4)-OV/CoPi	500 W Xe lamp with AM 1.5G filter	0.1 M Na2SO4 + 0.1M KPi	2.3 $mAcm^{-2}$ 1.23 V vs. RHE	10 h	*ACS Appl. Energy Mater. 4 (2021) 2864−2872*
$WO_3/BiVO_4$_Bi-PED.	100 $mWcm^{-2}$	0.5 M Na_2SO_4 + 0.1 M Na_2HPO_4 pH 7.0	2.1 $mAcm^{-2}$ 1.23 V vs. RHE	2 h	*Chem. Eng. J. 399 (2020) 125836*
$WO_3/BiVO_4/BiFeO_3$	100 $mWcm^{-2}$	0.5 M Na_2SO_4	1.5 $mAcm^{-2}$ 1.23 V vs. RHE	50 min	*ACS Appl. Energy Mater. 2 (2019) 6428−6439*
$WO_3/BiVO_4/TiO_2$/ FeOOHNiOOH	**100 $mWcm^{-2}$**	**0.5 M Na_2SO_4**	**4.6 $mAcm^{-2}$ 1.23 V vs. RHE**	**24 h**	**This work**